Daytime Tropical D-region Parameters from Short Path VLF Phase and Amplitude

Neil R. Thomson

Physics Department, University of Otago, Dunedin, New Zealand

Abstract

Observed phases and amplitudes of VLF radio signals propagating on a short (~300-km) path, are used to find improved parameters for the lowest edge of the (D-region of the) Earth's ionosphere. The phases, relative to GPS 1-sec pulses, and the amplitudes were measured both near (~100 km from) the transmitter, where the direct ground wave is very dominant, and at distances of ~300 km near where the ionospherically reflected waves form a (modal) minimum with the (direct) ground wave. The signals came from the 19.8 kHz, 1 MW transmitter, NWC, on the North West Cape of Australia, propagating ~300 km ENE, mainly over the sea, to the vicinity of Karratha/Dampier on the N.W. coast of Australia. The bottom edge of the mid-day tropical/equatorial ionosphere was thus found to be well-modeled by $H' = 70.5 \pm 0.5$ km and $\beta = 0.47 \pm 0.03$ km^{-1} where H' and β are the traditional height and sharpness parameters as used by Wait and by the US Navy in their Earth-ionosphere VLF radio waveguide programs. US Navy modal waveguide code calculations are also compared with those from the wave hop code of Berry and Herman [1971]. At least for the vertical electric fields on the path studied here, the resulting phase and amplitude differences (between the ~100-km and ~300-km sites) agree very well after just a small adjustment of ~0.2 km in H' between the two codes. Such short paths also allow more localization than the usual long paths; here this localization is to low latitudes.

1. Introduction

The D-region is the lowest altitude part of the Earth's ionosphere. By day, in this region, the neutral atmosphere is ionized mainly by solar EUV radiation and galactic cosmic rays. Low in the D-region, these down going ionizing sources have increasingly been absorbed by the increasing atmospheric density; also the electron recombination and attachment rates have become so high that the free electron density becomes very small. The lower D-region (~ 50-75 km) forms the rather stable upper boundary, or ceiling, of the Earth-ionosphere waveguide which is bounded below by the oceans and the ground. Very Low Frequency (VLF) radio waves (~2-40 kHz) travel over the Earth's surface in this waveguide. Observations of their propagation characteristics result in one of the best probes available for measuring the height and sharpness of the lower D-region. The (partial) ionospheric reflections of the VLF waves occur because the electron densities (and hence refractive indices) change rapidly (in the space of a wavelength) with height in this region, typically from less than ~1 cm^{-3} up to ~1000 cm^{-3}, near mid-day. These electron densities are not readily measured by means other than VLF. For higher frequencies, such as those used in incoherent scatter radars, the fractional change in refractive index, in the space of their much shorter wavelengths, results in much smaller, typically incoherently reflected, amplitudes from D-region heights compared with those from the more coherent VLF reflections. These higher frequency reflections thus tend to be too small and so masked by noise or interference. The air density at D-region heights is too high for satellites, causing too much drag. Rockets are expensive and transient; although some have given good results, there have generally been too few to cope with diurnal, seasonal and latitudinal variations.

Because VLF radio waves can penetrate some distance into seawater and, because they can be readily detected after propagating for many thousands of km, the world's great naval powers maintain a number of powerful transmitters to communicate with their submarines. The phase and amplitude of

the received signals provides a good measure of the height and sharpness of the lower edge of the D-region. The US Naval Ocean Systems Center (NOSC), developed computer programs (MODESRCH, MODEFNDR, LWPC - Long Wave Propagation Capability) which take the input path parameters, calculate appropriate full-wave reflection coefficients for the waveguide boundaries, and search for those modal angles which give a phase change of an integer multiple of 2π across the guide, taking into account the curvature of the Earth [e.g. *Morfitt and Shellman,* 1976; *Ferguson and Snyder*, 1990]. Further discussions of the NOSC waveguide programs and comparisons with experimental data can be found in *Bickel et al.* [1970], *Morfitt* [1977], *Ferguson* [1980], *Morfitt et al.* [1981], *Thomson* [1993], *Ferguson* [1995], *Cummer et al.* [1998], *McRae and Thomson* [2000, 2004], *Thomson and Clilverd* [2001], *Thomson et al.* [2005, 2007, 2009], and *Cheng et al.* [2006].

The NOSC programs can take arbitrary electron density versus height profiles supplied by the user to describe the D-region profile and thus the ceiling of the waveguide. However, from the point of view of accurately predicting (or explaining) VLF propagation parameters, this approach effectively involves too many variables to be manageable in our present state of knowledge of the D-region. As previously, we follow the work of the NOSC group by characterizing the D-region with a Wait ionosphere defined by just two parameters, the 'reflection height', H', in km, and the exponential sharpness factor, β, in km^{-1} [*Wait and Spies,* 1964]; the studies referenced in the previous paragraph also found this to be a satisfactory simplification. The LWPC version used here includes the modifications described by *McRae and Thomson* [2000] to assure that LWPC uses a full range of modes and electron densities (as does ModeFinder).

Daytime propagation is rather stable, potentially resulting in quite well-defined values of H' and β characterizing the lower D-region. NOSC recommended H' = 70 km and β = 0.5 km^{-1} for summer mid-latitudes (and by implication low latitudes) but H' = 72-75 km and β = 0.3 km^{-1} for winter mid-

latitudes [*CCIR,* 1990; *Morfitt,* 1977]. These parameters were derived from amplitude measurements only, mainly versus distance from aircraft flights lasting several hours. No account was taken of the changes in H' and β with solar zenith angle during the course of the day. These changes in H' and β with solar zenith angle were later measured and characterized by *Thomson* [1993] and *McRae and Thomson* [2000] by measuring amplitude and relative phase changes at fixed sites during the course of typical days. These authors obtained their value of H' = 70 km for summer mid-day, solar maximum, by measuring the amplitude at a fixed location near a modal minimum at a range of ~600 km over a mid-latitude, part-land, part-sea path [*Thomson,* 1993]. The technique was quite sensitive but depended on the transmitter radiated power (which was measured to only a moderate accuracy) and the conductivity of the ground, which though not a sensitive parameter, was rather uncertain. NOSC obtained their value of H' = 70 km for summer mid-day essentially from the positions (and amplitudes) of the (amplitude) modal minima on their flights at the times that the aircraft happened to travel through them. The values of β were essentially determined in both cases from the attenuation for the paths, assumed constant along the paths for NOSC, and to be varying with solar zenith angle for *Thomson* [1993] and *McRae and Thomson* [2000].

Here, not only amplitude, but also phase change measurements with distance along the path are used to determine more accurate values of H' and β. A short 300 km low latitude (~20°) path is used. This has the advantage of giving localized values of H' and β with the solar zenith angle essentially not changing along the path. It might appear that such rather local measurements could also be a disadvantage. However, as discussed later the values of H' and β so found can be expected to apply at least within ±30° latitude of the geomagnetic equator (where the ionizing effects of the incoming galactic cosmic radiation are least). There has also been some uncertainty as to whether modal

waveguide codes give sufficient accuracy at such short distances; so a check is made against results from the wave hop code of *Berry and Herman* [1971].

2. VLF Measurement Technique: phase in particular

2.1 The Portable VLF Loop Antenna and Receiver

For all the phase and amplitude recordings made in N.W. Australia reported here, the VLF signals (from NWC on 19.8 kHz) were received on a portable loop antenna (60 turns of ~1.0 mm diameter copper wire, with rectangular sides ~0.50 m x 0.58 m in a plywood frame). All the circuitry was battery powered and carefully shielded, positioned and checked so that any feedback from the receiver electronics back into the loop was negligible. To assure that the receiver was fully sensitive to the magnetic field of the incoming wave, as intended, and negligibly sensitive to the wave's electric field, the loop was connected to the receiver electronics via a small transformer with primary center-tapped to ground (accurately assured by bifilar winding). As an additional precaution, all phase and amplitude measurements were taken in pairs: first with the loop pointing directly 'towards' the transmitter and then, after rotation by 180° about the vertical, pointing directly 'away' from the transmitter, thus reversing the phase of the magnetic field but not the phase of any (residual) electric field. The two resulting amplitude measurements in each pair seldom differed by more than ~0.3 dB, usually less; similarly, the two resulting phase measurements in each pair seldom differed by more than ~0.5 μs, usually less.

NWC, as for other US Navy VLF transmitters, is modulated with 200 baud MSK. Its center frequency is 19.8 kHz. This means that, during each 5 ms period, the transmitter is transmitting one of four sine waves: two available frequencies, 19.75 kHz and 19.85 kHz each available as two sine waves 180° out-of-phase with each other. This means effectively that, when NWC has transmitted one of

these sine waves for 5 ms, it can, with no jump in phase, either change to the appropriate sine wave on the other frequency for the next 5 ms or continue transmitting the same wave for the next 5 ms. This allows one bit change per 5 ms or 200 bit changes per second which is 200 baud. MSK viewed in this way has been discussed in more detail by *Thomson* [1981, 1985].

The loop antenna receiver has a simple internal crystal oscillator from which VLF frequencies, such as 19.75 kHz and 19.85 kHz, are synthesized as selected by front panel switches. The receiver electronics then phase-locks the internally synthesized frequency to the appropriate (i.e. the same) incoming VLF frequency. The receiver is thus a type of homodyne receiver. There has, of course, always been a concern with homodyne receivers that some of the local oscillator (e.g. the internally generated 19.75 or 19.85 kHz here) will get picked up by the (loop) antenna and amplified by the receiver. However, this effect is much more manageable at VLF than HF, and with careful design, layout and shielding, the self-pick-up was able to be made negligible even to the high accuracy required here. It is probably worth also noting that the MSK modulation with its two 180° reversed phases on each frequency is helpful both in dealing with the potential feedback problem and in assessing when it has been avoided, as is the 180° reversal of the loop antenna direction for each pair of measurements described above. The phase-locking method used is broadly similar to that described by *Thomson* [1981, 1985] except that the crystal is used here as a standard VCXO where the analogue phase/frequency is adjusted continuously by the voltage controlled capacitance of a reverse biased diode, rather than in small digital steps in a digital synthesizer.

The amplitude is extracted from the output of the phase sensitive detectors and, after filtering, diode detection and some additional filtering is displayed on an analogue meter attached to the portable loop. The analogue meter was preferred to a digital meter for rejecting sferics by eye and for rapid orientation of the loop towards a maximum. The amplitude measurements were recorded by hand for

later analysis. Each individual measurement typically took less than a minute. The calibration (effectively the gain) was checked periodically using a signal generator and digital oscilloscope and has been confirmed to be rather constant over long periods (years). Measurement of the (fixed) effective loop area and inductance enabled the meter to be calibrated in terms of wave field strength. The units chosen were μV/m because these have been those most commonly used for this purpose, even though the loop, of course, is not actually directly measuring the (vertical) electric field, E_z, but is really responding to the (horizontal) magnetic field, B_y, of the wave. For most purposes, particularly for propagation over distances greater than several hundred km, due to the fact that normally $E/B = c =$ the constant speed of light, it does not matter. However, in our case here, because the propagation distances are less than a few hundred km, this issue will be revisited later. None-the-less, all electric field amplitudes (in μV/m) given in this paper (whether calculated or measured) will, if divided by c, the speed of light, give the true magnitude (calculated or measured) of the (horizontal) magnetic field of the wave. Although the portable loop and its receiver are so calibrated to read in μV/m, this calibration is not actually fully necessary here because in reality it is the ratios of the amplitudes at ~300 km and ~100 km from the transmitter that are effectively used.

The phase of the incoming VLF MSK signal is effectively measured by measuring the phase of the local oscillator sine wave locked to the incoming signal. The VLF phase meter measures and displays the time in μs (to 0.1 μs) between the GPS 1-s pulse (from a Trimble Lassen SQ GPS receiver) to the next positive zero-going crossing of the (phase-locked) local oscillator sine wave. Again a single such measurement can usually been made within about a minute (at the same time as an amplitude measurement), provided the GPS unit has previously been used not too far (~100 km or so) from the current site, and so does not have to determine its position afresh from scratch. Again the readings are integrated by eye and recorded by hand for later analysis. The phase measurements are always

modulo half a cycle (corresponding to an ambiguity of 180°) because of the MSK modulation, but this was normally of little consequence here.

Most of the portable loop phase and amplitude measurements used here were recorded in public parks (sports grounds). North-West Australia has truly vast tracts of open space where there are no electric power lines, no phone lines, no buried (man-made) metal objects etc. Quite a number of measurements were made in such places and used as interference-free references. However, convenience, particularly traveling distance and time, meant that most of the measurements were made in/near the towns typically in parks or nearby convenient vacant land. Hence care, as always, was needed, particularly in the parks to keep sufficiently away from (buried) power lines and the like, particularly checking that measurements were self-consistent over distances of at least a few tens of meters and from one (nearby) site to the next. Some sites tried needed to be rejected but most, provided certain parts were avoided, proved satisfactory and convenient.

2.2 The Fixed VLF Recorders

NWC, like other US Navy VLF transmitters, typically has very good phase and amplitude stability. However, as with the other US transmitters, it normally goes off-air once a week for 6-8 hours for maintenance. On return to air, the phase is still stable but the value of the phase (relative to GPS or UTC) is often not preserved. In addition, in the course of a typical week, there may be some gradual phase drift or a small number of additional times when there are random phase jumps. It is thus very desirable to have a fixed recorder continuously recording while the portable measurements are made. This was not convenient to do in N.W. Australia but was readily done in Dunedin, New Zealand, 5.7 Mm away, where the signal-to-noise ratio is still very good. Because of the stability of the (daytime) propagation this provided a satisfactory method of checking for and, when necessary, compensating

for, any such phase drifts or jumps. The recorders used, for both phase and amplitude, were SoftPAL and AbsPAL receivers [*Dowden and Adams*, 2008; *Thomson et al.,* 2005, 2007, 2009; *McRae and Thomson,* 2000, 2004, and references therein]. In particular, two SoftPAL receivers recorded amplitude and phase (with respect to GPS 1-second pulses) from two independent VLF receivers and antennas (one loop and one vertical electric field) at Dunedin.

3. VLF Measurements and Modeling Comparisons

3.1 The Paths

Figure 1 shows the location of the NWC transmitter, the principal receiving locations and the paths. It can be seen that the short (~100 km) path to Onslow is clearly all-sea while the longer (~300 km) paths are mainly over the sea especially in the case of the Dampier path which is virtually all-sea.

3.2 N.W. Australia Observations during October 2009 compared with Modeling using B_y from ModeFinder

Most of the VLF waveguide propagation programs, such as the US Navy's ModeFinder and LWPC, are set up (primarily) to calculate the vertical electric field (E_z) amplitudes and phases along the path. However, observations are more commonly made by measuring the horizontal magnetic field of the wave, B_y, (perpendicular to the direction of propagation, x) because the gains of the loop antennas used for the measurements are much less sensitive than electric field antennas to changing environmental factors such as the wetness of nearby trees and moving animals or plants. However, such loop antenna field strengths are still usually expressed (calibrated) in V/m effectively by using $E_z = cB_y$. For the vast majority of cases in the Earth-ionosphere waveguide, this is a totally satisfactory approximation. However, for the ionospherically reflected part of the wave close to the transmitter, this may not be appropriate. For example, for the wave of a down-going ray with $E_w = cB_w$ reflecting at 45° from perfectly conducting ground, the horizontal magnetic field measured (by a loop) at the ground would be $2B_w$, resulting in a reading of $E_z = 2cB_w$, while a (vertical) electric field antenna would measure $2E_w\cos 45^o = \sqrt{2}cB_w$, different by a factor of $\sqrt{2}$ or 3 dB. At a distance of 100 km from the transmitter, this factor is slightly greater (due to the arrival angle being slightly further from the horizontal) but the ionospherically reflected amplitude is only ~15% of the ground wave amplitude (in

B_y) which means that the difference between using B_y as opposed to E_z turns out to be only ~0.5 dB which is minor but not quite negligible.

At a distance of 300 km, the difference between using B_y and E_z is reduced by the ionospheric wave effectively arriving at a much smaller angle with the ground, but increased by the ionospheric wave now being nearly comparable in size with the ground wave and destructively interfering with it. Hence, it was felt clearly desirable to calculate B_y rather than the usual E_z so as to match with the B_y measurements of the portable loop. ModeFinder was used for this because it was found to be simpler to add this B_y option to the ModeFinder code than to the much larger LWPC code. As mentioned in the introduction, the two codes give essentially the same results (for E_z) provided they are both set so as not to cut off high order modes or low electron densities. LWPC has clear advantages for longer paths because it is set up to cope with changing parameters along the paths (particularly changing geomagnetic dip and azimuth). For our short 300 km path here, these potential advantages are not needed. It is also worth mentioning that many modes are needed for short distances such as the 100 km and 300 km used here. Typically the waveguide codes produced about 17 modes with the higher order modes having attenuations up to ~300 dB/Mm (and so up to ~30 dB over 100 km) and phase velocities up to ~3*c*. In comparison the least attenuated modes (the well-excited first order modes) had attenuations of ~1 dB/Mm and phase velocities very close to *c*.

Before comparing the modeling calculations with the observations, some features of the observations, including adjustments for transmitter (NWC) phase drifts need to be discussed. Figure 2 shows the phases and amplitudes of NWC at Dunedin, NZ (5.7 Mm away) recorded while the portable loop phase and amplitude measurements were being made in N.W. Australia. The Dunedin amplitude plot (in dB above an arbitrary level) shows a spread of only a few tenths of a dB, apart from the small solar flare near path mid-day on 25 Oct 2009. This stability of path is typical for the summer half of

the year. The Dunedin phase plot (referenced to GPS 1-sec pulses) appears less stable: the 0.3 dB spread in amplitude is only ~4%, but 4% of a radian is ~2°, much less than the day-to-day phase drifts even after ignoring the small solar flare on 25 Oct 2009 and the 90° phase jump at ~0130 UT on 24 Oct 2009 (a minor Dunedin instrumental effect which will be discussed later). As will be seen shortly, the day-to-day phase drifts occurred at the transmitter, not on the NWC-Dunedin path, and can be readily allowed for using this Dunedin phase plot.

Over 20 sets of portable loop phase and amplitude measurements on the NWC signals were made at Onslow spread over the 3 days 21-23 Oct 2009. All the measurements were made within 3-4 hours of mid-day, mainly within 2 hours. Seven sites were used with ranges from the transmitter of ~93-100 km. All the phase measurements were entered into an (Excel) spreadsheet together with the site locations measured by a portable GPS receiver and later checked against Google Earth. The spreadsheet was used to adjust the measured phase delays for the different ranges from the transmitter (1.0 μs per 300 m) to allow comparison of sites. The agreement between sites on each of the days was very good (within a few tenths of 1 μs). All sites were judged to be satisfactory. Table 1 shows one representative measurement set from each of the 3 days, all from the same site (at a range of 100.16 km). As mentioned previously, each set included four phase measurements. For each day, the table shows the average of the two 180° loop orientations for each of the two (sideband) frequencies.

The second last column of the table shows the phase recorded at Dunedin from Figure 2 (modulo 90° in the case of 21 Oct 09; this is discussed in section 4.1). The last column shows the Dunedin phase (in degrees) adjusted in line with the phases of NWC observed at Onslow as shown in columns 3 and 4. For example, the mean Onslow phase on 21 Oct 09 was (9.5 + 2.8)/2 = 6.1 μs, while on 22 Oct 09 it was (3.8 + 15.5)/2 = 9.6 μs. This (apparent) increase in phase delay of 9.6 – 6.1 = 3.5 μs from 21 to 22 Oct 09 is equivalent to a lowering of the phase angle by 3.5 x 19800 x 360 = 25°; thus the "deg

adj." for 22 Oct 09 is –27 + 25 = -2° as shown. Thus the phase change of -2° - (-48°) = 46°, seen at Dunedin 21-23 Oct 09 in Figure 2, is virtually all accounted for by NWC phase drift rather than path changes. This further illustrates the stability of the NWC-Dunedin path, at least during the (near) summer months, and so the value of the Dunedin monitoring for keeping track of NWC's phase at source.

The amplitude of the NWC signal at Onslow (only 100 km away) is very high (97 mV/m in October 2009), higher than the portable loop receiver was initially designed for. This was dealt with by reducing the gain at Onslow by replacing the two 39 Ω resistors usually used in series with the loop coil with two 2.0 kΩ resistors. The resulting gain change and phase shift was readily calculated (using the measured loop inductance) and confirmed in the field at Karratha (where the mid-day field strength is ~10 mV/m) by alternating the gains over a few minutes. So, the last line of Table 1 gives the phase at the principal site in Onslow corrected to the standard loop set-up of 2 x 39 Ω for comparison with all the other measurements (in the Karratha/Dampier region) which were measured with this standard set-up (i.e. with 2 x 39 Ω).

Table 2 shows representative values of the phase measurements made at the principal site in Karratha (Millars Well Oval, 299.90 km from NWC) near mid-day (~1200 LT = ~0400 UT). There were 3 days on which measurements were made: 20, 24 and 25 Oct 2009. The results from some nearby sites were again entered into a spreadsheet similar to that for Onslow to check for consistency. This was slightly complicated by Karratha being close to (slightly beyond) a modal minimum. Calculations and observations showed that ~30 mV/m of ground wave was (destructively) interfering with ~20 mV/m of ionospherically reflected waves to give ~10 mV/m of observed signal. However, apart from needing to reject one (park land) site due to interference/buried conductors, it became clear the Millars Well Oval (and a closely neighboring site) were giving reliable results. At first it was

thought that locating the position and depth of the amplitude modal minimum, 10-30 km on the NWC side of Millars Well might produce the best results. However, the minimum is fairly broad and this involved too much traveling time and so was not fully pursued; using phase and amplitude near Millars Well turned out to be more efficient.

In Table 2, as in Table 1, the final column (the Dunedin phase corrected by the phase measured in N.W. Australia) is a measure of path stability. Clearly there is a spread of ~±10° at Karratha compared with a total spread of ~2° at Onslow. The NWC-Dunedin stability is likely good in both cases; so this increased spread on the NWC-Karratha path will be due to the increased proportion of the ionospheric component at Karratha compared with Onslow, and also the effect of the partial canceling near the modal minimum at Karratha. None-the-less the error on the mean phase at Karratha is probably only ~±7° (~±1.0 μs), which is fairly satisfactory.

The mean Onslow and Karratha phases (last lines in Tables 1 & 2) were then used, in Table 3, to find the observed phase delay difference between Onslow and Karratha. This required correcting for the phase changes at NWC (as measured at Dunedin) between the times of the Onslow and Karratha measurements as shown in the table. Also, as already mentioned, the phase meter measures modulo half-a-cycle, so, for convenience, half a period (25.3 μs) of NWC's 19.8 kHz has been added just to make the delay difference positive.

This delay difference (between Onslow and Karratha) can be thought of as consisting of two parts: the free space part along the surface of the Earth and the ionospherically reflected part. Indeed programs such as ModeFinder and LWPC output their phases relative to the free-space delay. Table 4 shows the locations of NWC and the principal sites used in each of Karratha and Onslow (using Google Earth and a portable GPS receiver). The distances in rows 2 & 3 were calculated using the Vincenty algorithm [*Vincenty*, 1975; www.ngs.noaa.gov/cgi-bin/Inv_Fwd/inverse2.prl;

www.ga.gov.au/geodesy/datums/vincenty_inverse.jsp] and from these the delays were found using the speed of light, c = 299.792458 m/μs. The difference between the NWC-Karratha and NWC-Onslow delays, 666.3 μs, was then reduced by an integral number of half cycles: 666.3 – 26 x 0.5/0.0198 = 9.7 μs, to allow for the phase measuring half-cycle ambiguity. This free space delay was then subtracted from the observed delay giving the waveguide part of the delay difference between Onslow and Karratha, 14.3 - 9.7 = 4.6 μs ≡ 33° which was then subtracted from the 42° calculated by ModeFinder for the phase of NWC at Onslow giving 9° for the 'observed' phase at Karratha shown in the top panel of Figure 3.

The average measured amplitudes of NWC at Millars Well, Karratha and at Onslow were 80.8 dB and 99.7 dB, respectively, above 1 μV/m. The ModeFinder calculated NWC amplitude at Onslow (for 1 MW radiated) was 100.0 dB above 1 μV/m, 0.3 dB greater than that observed. Hence the observed amplitude at Karratha for 1 MW radiated would have been 80.8 + 0.3 = 81.1 dB above 1 μV/m; this is the 'observed' amplitude shown in the 2nd panel of Figure 3. Also shown in the top two panels of Figure 3 are ModeFinder calculations for B_y at Karratha (expressed as dB > 1 μV/m using $E_z = cB_y$) for NWC radiating 1 MW for appropriate values of H' and β over an all-sea path. It can be seen that the best fit to the observations is obtained with H' = 70.4 km and β = 0.465 km^{-1}. These values were used (retrospectively) in ModeFinder to calculate the phase (42°) and amplitude (100.0 dB) at Onslow above. This procedure required only one iteration because the ionospheric part of the signal at Onslow is only ~15% of the total at Onslow while it is effectively more than 100% at Karratha due to the modal minimum there.

As was seen in the top panel of Figure 1, the NWC-Karratha path is not all over the sea; about 1/3 is over land. According to estimates made by *Morgan* [1968] for the US Navy and incorporated into LWPC, the VLF ground conductivity in the region is expected to be fairly low, ~0.001 S/m.

Unfortunately the ModeFinder code, which was needed to get B_y, makes no provision to segment the 300 km path with the first 200 km as all-sea conductivity (~4 S/m) and the last 100 km as (0.001 S/m) land. However, LWPC can do this, but only for the fairly similar E_z case. By doing appropriate runs with LWPC (and so E_z), it was found that 300 km of 0.01 S/m land gave very nearly the same results as 200 km of sea plus 100 km of 0.001 S/m land. So a B_y run was made with ModeFinder with 300 km of 0.01 S/m land and the results are shown in the bottom two panels of Figure 3. It can be seen that this would raise *H'* to 71.0 km (from 70.4 km in the all-sea case), while β would hardly change.

It should not however immediately be thought that this lower conductivity will give the better value of *H'*. The ground conductivities are difficult to assess accurately; they are just estimates. Generally for normal land worldwide, conductivities tend to range ~ 0.01 S/m to 0.001 S/m. Further, and significantly, these estimates are made on distance scales of at least 50-100 km, while the land part of the path into Karratha is only ~10 km (<~λ at 19.8 kHz)) from the sea with the land altitude averaging little more than 10 m; proximity and salt from the sea are thus likely to be significant in raising the effective conductivity. This issue is considered further in section 3.3.

3.3 Observations at Dampier during October 2009 compared with Modeling using B_y from ModeFinder

As can be seen in Figure 1, the NWC-Dampier path is attractive because it is virtually all-sea. However, fewer measurements were made near Dampier due to geographic, time and roading constraints. Measurements were made on just 2 days, 24 & 25 Oct 2009, and at just two sites, Hampton Oval (292.57 km from NWC and chosen as the principal site with parameters tabulated below) and Dampier Sports Oval (25 Oct 2009 only) which was ~1 km further from NWC than Hampton Oval. The relevant phase measurements for Hampton Oval, Dampier, are shown in Table 5

(similar to those for Millars Well, Karratha, in Table 2). As for the Karratha observations, the phases measured at the two Dampier sites were entered into a spreadsheet and gave good agreement when allowance was made for their different distances from NWC.

Table 6 shows how the observed phase difference between Dampier and Onslow was determined using the same procedure that was used in Table 3 for Karratha and Onslow. Table 7 shows the free-space phase differences for Dampier-Onslow calculated in the same way as for Karratha-Onslow in Table 4. The waveguide only part of the delay is then shown calculated as before and this 13° is subtracted from the ModeFinder calculated phase of 42° at Onslow to give the 'observed' 29° at Dampier shown in Figure 4 which compares ModeFinder calculated (B_y) phases and amplitudes at Dampier with observations in the same way as in Figure 3 for Karratha. Three horizontal lines are shown for the 'observed' amplitude in the lower panel of Figure 4 because, although the phases at the two Dampier sites agreed well with each other, the amplitudes at the two sites did not. The highest "observed" amplitude line represents the amplitudes measured at Hampton Oval while the lowest is for the other site, Dampier Sports Oval. Both of these sites were near the shore, showed signs of reclamation work and exhibited amplitude variations across the site which were somewhat greater than normal. Readings from additional nearby sites would have been desirable but insufficient time was available to locate such suitable sites. On balance it seemed that the Hampton Oval site was slightly more likely to be reliable, but only slightly; so a mean amplitude was chosen by weighting the two sites 2:1, giving the central 'observed' amplitude line. As can be seen, the best fit is for H' = 70.4 km and β = 0.48 km^{-1}. This would be most consistent with the results from the NWC-Karratha path in section 3.2 if that path is effectively taken as nearly all-sea too, as already suggested there.

3.4 E_z Comparisons: LWPC, Wave Hop and Observations

In the top two panels of Figure 5 the NWC observations at Karratha are compared with LWPC's standard (E_z) output. A comparison with the B_y output in Figure 3 shows the differences are neither large nor negligible. In particular, for example, the amplitude minima of the $\beta = 0.46$ and 0.50 curves shows them to be lower in the B_y plot than in the E_z plot by ~1.5 dB. As can be seen, the top (E_z) panels of Figure 5, if used, would have implied $H' = 70.25$ km and $\beta = 0.50$ km^{-1} as compared with the values $H' = 70.4$ km and $\beta = 0.465$ km^{-1} already concluded from the corresponding B_y panels of Figure 3 (because the loop observations were fundamentally B_y measurements). The difference, though not great, is none-the-less not quite negligible.

These LWPC E_z results also make it possible to make a direct comparison with (a slightly modified version of) the wave hop code of *Berry and Herman* [1971] which also outputs E_z. This is done in the bottom two panels of Figure 5 where the LWPC results from the top panels have been moved to the left by 0.2 km (shown dotted) to enable a closer comparison. The agreement between LWPC and the wave hop code is remarkably good subject to the issues already mentioned (the 0.2 km shift, the necessity of LWPC being set-up to use a full range of modes and not to cut-off its electron density versus height profile) and one further puzzling, though probably not serious issue, namely a phase difference of ~135°. Part of this difference, 90°, is probably associated with whether the (E_z) output phase is relative to the phase of the antenna current or the phase of the electric field very near the antenna. The remaining ~45° seems harder to account for. None-the-less, the very good basic agreement between the very different waveguide and wave hop codes encourages confidence in their use in determining the ionosphere parameters (H' and β) from short path experimental VLF phase and amplitude observations.

3.5 Winter (June, 2008): H' and β at Karratha from Observations and ModeFinder B_y Modeling

Phase and amplitude observations (similar to those already described for October 2009) were also made near mid-day at Millars Well, Karratha, and Onslow in June 2008 (mid-winter). The results, following a similar process to that for the October 2009 data in section 3.2, are shown in Figure 6. The only significant difference was that the transmitter was much more phase stable (varying only 0.4 μs ≡ 3° over the 3 days, 26-28 Jun 08, in Onslow) than for the 2009 measurements. This meant that the NWC-Dunedin path was not needed for phase drift corrections, which was fortunate as the path in June was less phase stable (fairly typical of winter conditions) than in October. It can be seen that Figure 6 is showing that, in winter, at mid-day when the solar zenith angle is ~45°, at Karratha, H' = 72.1 km and $\beta = 0.405$ km^{-1}.

4. Discussion, Summary and Conclusions

4.1 Phase Ambiguities

As discussed in section 2.1, MSK is a continuous-phase modulation (no phase jumps) but none-the-less MSK phase measurements generally involve an ambiguity of 180° because each of the sideband frequencies (19.75 and 19.85 kHz in the case of NWC) can be transmitted in either of two phases, each 180° out-of-phase with the other. The portable phase meter used here always has the 180° ambiguity because of frequent turning off and on. (No permanent time record of the modulation switching pattern is kept.) Recorders can, in principle, track phase changes without 180° (or 360°) ambiguities provided the transmitter, receiver and recorder operate continuously, and the signal to noise ratio is always good. However, if a recorder outputs just one phase at a time (rather than one for each of the sideband frequencies), as our recorders do, and some discontinuity causes the phase of one (only) of the sideband frequencies to change by 180°, then the resulting (mean) output phase will change by 90°. An example of this can be seen in Figure 2 at ~0130 UT 24 October 2009. Thus phase ambiguities of

90° are possible with the Dunedin recorders; sometimes they are resolvable (ie the ambiguity remains at 180°) and sometimes they are not (ie the phase ambiguity really has been reduced to 90°). In the case of the period 22-25 Oct 2009, it appeared fairly certain that the only (90°) jump was resolvable leaving only the usual 180° ambiguity. In the case of the period 21-22 Oct 2009, the phase discontinuities (at night on 21 Oct 2009) could not be reliably resolved so the recorder phase for 21 Oct 2009 (daytime) was shifted by n x 90° = 1 x 90° = 90° to get the best fit in Table 1. This did not matter because the period 22-25 Oct 2009 enabled the Onslow phase of 22-23 Oct to be linked to the Karratha phase of 24-25 Oct with the better ambiguity of 180°

Effectively an ambiguity of 180° in Figure 3 is no ambiguity at all because there are no heights anywhere near 70.5 km, other than ~70.5 km itself, where the calculations could match the amplitude and phase observations with phase shifts of an integral multiple of 180°. Although, as discussed in the last paragraph, a phase ambiguity of just 90° is unlikely here, such an ambiguity could give a near match in Figure 3 (though not in figure 4) for heights around 72-73 km. These heights can be largely ruled out both by Figure 4 and by the earlier work of *Thomson* [1993] and the US Navy, discussed in the introduction, which found that, for the sun near the zenith, as here in October, H' = 70 km with a likely error of ~±1 km and no more than ±2 km. In addition, *Thomson* [1993] showed that when the sun is ~45° from the zenith, as for the (winter) results of Figure 6, H' is ~1.5 km higher than for (near) overhead sun, which agrees well with the results of Figure 6 where it can be seen that no 90° shift could give any agreement between calculations and observations other than that shown.

4.2 Comparison with Other Observations, Discussion and Conclusions

Figures 3 and 4 (for the 300 km tropical paths NWC to Karratha/Dampier), for late October 2009, give H' = 70.5 km and β = 0.47 km^{-1}. From the discussion on the last column of Table 2 in section 3.2,

the (random) error in the mean phase measurement of NWC at Karratha was ~ ±7°. This is likely to be principally due to random variations in the ionospherically reflected part of the signal there being effectively magnified by partial destructive interference with the (direct and more stable) ground wave. Of course, the phase difference between Karratha and Onslow, which determines the "observed" phase in Figure 3, also depends on the phase measurements at Onslow. From the last column of Table 1 it can be seen that the scatter over the 3 days of Onslow observations is quite small, ~±1°. This is consistent with the NWC to Dunedin path (used to correct for NWC phase drifts) being rather stable in October (as is also the stability of NWC's amplitude seen at Dunedin in Figure 2). This greater stability of the NWC-Dunedin path as compared with the shorter NWC-Karratha path is likely to be partly due to the destructive interference at Karratha just mentioned and partly due to the well-known observed better phase stability of long VLF paths which seems, in turn, to be partly due to the effective averaging along the long paths and partly due to low sensitivities associated with the near grazing reflection (or high incidence angles) and the resulting single-mode propagation. A conservative estimate of the total observed phase error for Karratha/Dampier would thus be ~ ± 10° which, from figures 3 and 4, corresponds to ~ ± 0.5 km in *H'*. Similarly the observed amplitude error of ~ ± 1.0 dB for Karratha (or ± 1.5 dB at Dampier), as compared with Onslow, results, from Figures 3 and 4, in a likely error of ~ ± 0.03 km^{-1} in β. Hence, for this low latitude path, the results here give *H'* = 70.5 km ± 0.5 km and β = 0.47 ± 0.03 km^{-1} for near overhead sun (< 10° from the zenith).

As discussed in the introduction, for (near) overhead sun, *Thomson* [1993] found *H'* = 70 km and β = 0.45 km^{-1} at solar maximum while NOSC found *H'* = 70 km and β = 0.5 km^{-1} for 'summer'. The current results for 2009 are, however, for solar minimum where *McRae and Thomson* [2000] found *H'* = 70.7 km and β = 0.39 km^{-1}. However, this lower β at solar minimum is likely to be due to the increased galactic cosmic rays at solar minimum increasing the mid-latitude electron density at heights

in the lower part of the VLF reflection height range relative to the (slightly reduced) Lyman-α ionization in the upper part of this height range [*Thomson and Clilverd*, 2001]. These effects will be much less at low latitudes where the (near) horizontal geomagnetic field significantly reduces the cosmic ray intensity [e.g. *Heaps*, 1978]. Hence the present low latitude results, though at solar minimum, should, in retrospect, be compared with the earlier (low to mid-latitude) solar maximum results. Thus the new results here, at solar minimum, although not consistent with the previous solar minimum results at general mid-latitudes, are consistent with the much lower cosmic ray intensities expected at low latitudes (or at solar maximum).

The higher solar zenith angle (45°, winter) results of Figure 6, H' = 72.1 km and β = 0.41 km^{-1}, are also reasonably consistent with the earlier solar maximum results of *Thomson* [1993], H' = 71.6 km and β = 0.41 km^{-1}.

The short-path (~300 km) phase and amplitude technique used here provides good accuracy for lower D-region electron number density parameters on a local scale without having to effectively average along long (many Mm) paths. None-the-less the results of *Heaps* [1978] for the variation of cosmic ray intensity with latitude imply that the apparently localized results here are likely to be valid for all (tropical) geomagnetic latitudes up to ~ $\pm 30^o$. This new short-path phase and amplitude technique can also be expected to be useful, in the future, for more accurately determining the variations in the D-region with latitude (due to cosmic rays etc) especially at higher geomagnetic latitudes where long (geomagnetically uniform) paths are hard to find.

Acknowledgements

The author is very grateful to his colleague, David Hardisty, for his design, development and construction of the VLF phase meter. Thanks also to http://rimmer/ngdc.noaa.gov of NGDC, NOAA, US Dept. of Commerce, for the digital coastal outline data and to english.freemap.jp for their free outline map of Australia, both used in Figure 1.

References

Berry, L.A. and J.E. Herman (1971), A wave hop program for an anisotropic ionosphere, *OT/ITS Research Rep. 11,* U.S. Dept. of Commerce, Boulder, CO.

Bickel, J. E., J. A. Ferguson, and G. V. Stanley (1970), Experimental observation of magnetic field effects on VLF propagation at night, *Radio Sci. 5***,** 19-25.

Dowden, R.L. and C.D.D. Adams (2008), SoftPAL, Proceedings of the 3rd VERSIM Workshop, Tihany, Hungary, 15-20 September 2008.

CCIR (1990). *Radio propagation and circuit performance at frequencies below about 30 kHz.* Document 6/1030-E (30 October 1989), *Report 895-1, Mod F, 29 pp,* XVII Plenary Assembly, Dusseldorf.

Cheng, Z., S. A. Cummer, D. N. Baker, S. G. Kanekal (2006), Nighttime *D* region electron density profiles and variabilities inferred from broadband measurements using VLF radio emissions from lightning, *J. Geophys. Res., 111,* A05302, doi:10.1029/2005JA011308.

Cummer, S. A., U. S. Inan, and T. F. Bell (1998), Ionospheric *D* region remote sensing using VLF radio atmospherics, *Radio Sci., 33*(6), 1781-1792.

Ferguson, J. A. (1980), Ionospheric profiles for predicting nighttime VLF/LF propagation, *Naval Ocean Systems Center Tech. Rep. NOSC/TR 530, NTIS Accession.ADA085399*. Natl. Tech. Inf. Serv. Springfield, VA 22161, USA.

Ferguson, J. A. (1995), Ionospheric model validation at VLF and LF, *Radio Sci.*, *30*(3), 775-782.

Ferguson, J. A. and F. P. Snyder (1990), Computer programs for assessment of long wavelength radio communications, version 1.0: full FORTRAN code user's guide, *Naval Ocean Systems Center Tech. Doc. 1773, DTIC AD-B144 839*, Def. Tech. Inf. Cent., Alexandria, Va.

Heaps, M.G. (1978), Parameterization of the cosmic ray ion-pair production rate above 18 km. *Planet. Space Sci.*, 26, 513-517.

McRae, W. M. and N. R. Thomson (2000), VLF phase and amplitude: daytime ionospheric parameters, *J. Atmos. Sol.-Terr. Phys.,* 62(7), 609-618.

McRae, W. M. and N. R, Thomson (2004), Solar flare induced ionospheric D-region enhancements from VLF phase and amplitude observations. *J. Atmos. Sol.-Terr. Phys.,* 66(1) 77-87.

Morfitt, D.G. (1977), Effective electron density distributions describing VLF/ELF propagation data,.*Naval Ocean Systems Center Tech. Rep*., *NOSC/TR 141, NTIS Accession ADA047508*, Natl. Tech. Inf. Serv. Springfield, VA.

Morfitt, D. G. and C. H. Shellman (1976), MODESRCH, an improved computer program for obtaining ELF/VLF/LF mode constants in an Earth-Ionosphere Waveguide. *Naval Electr. Lab. Cent. Interim Rep. 77T, NTIS Accession ADA032573*, Natl. Tech. Inf. Serv., Springfield, VA.

Morfitt, D.G., J.A. Ferguson, and F.P. Snyder (1981), Numerical modeling of the propagation medium at ELF/VLF/LF, *AGARD Conf. Proc., 305*(32*)*, 1-14.

Morgan, R.R. (1968), World-wide VLF effective-conductivity map, Westinghouse Report 80133F-1, NTIS product code AD675771.

Pappert, R. A. and L. R. Hitney (1988), Empirical modeling of nighttime easterly and westerly VLF propagation in the Earth-ionosphere waveguide, *Radio Sci. 23***,** 599-611.

Rhoads, F.J. and W.E. Garner (1967), An investigation of the modal interference of VLF radio waves, *Radio Sci.,2*(6), 539-546.

Thomson, N.R. (1981) Whistler-mode signals: spectrographic group delays. *J. Geophys. Res.*, 86(A6): 4795-4802, 1981.

Thomson, N. R. (1985), Reflection of VLF radio waves from distant mountain ranges, *J. Atmos. Terr. Phys., 47*, 353-362.

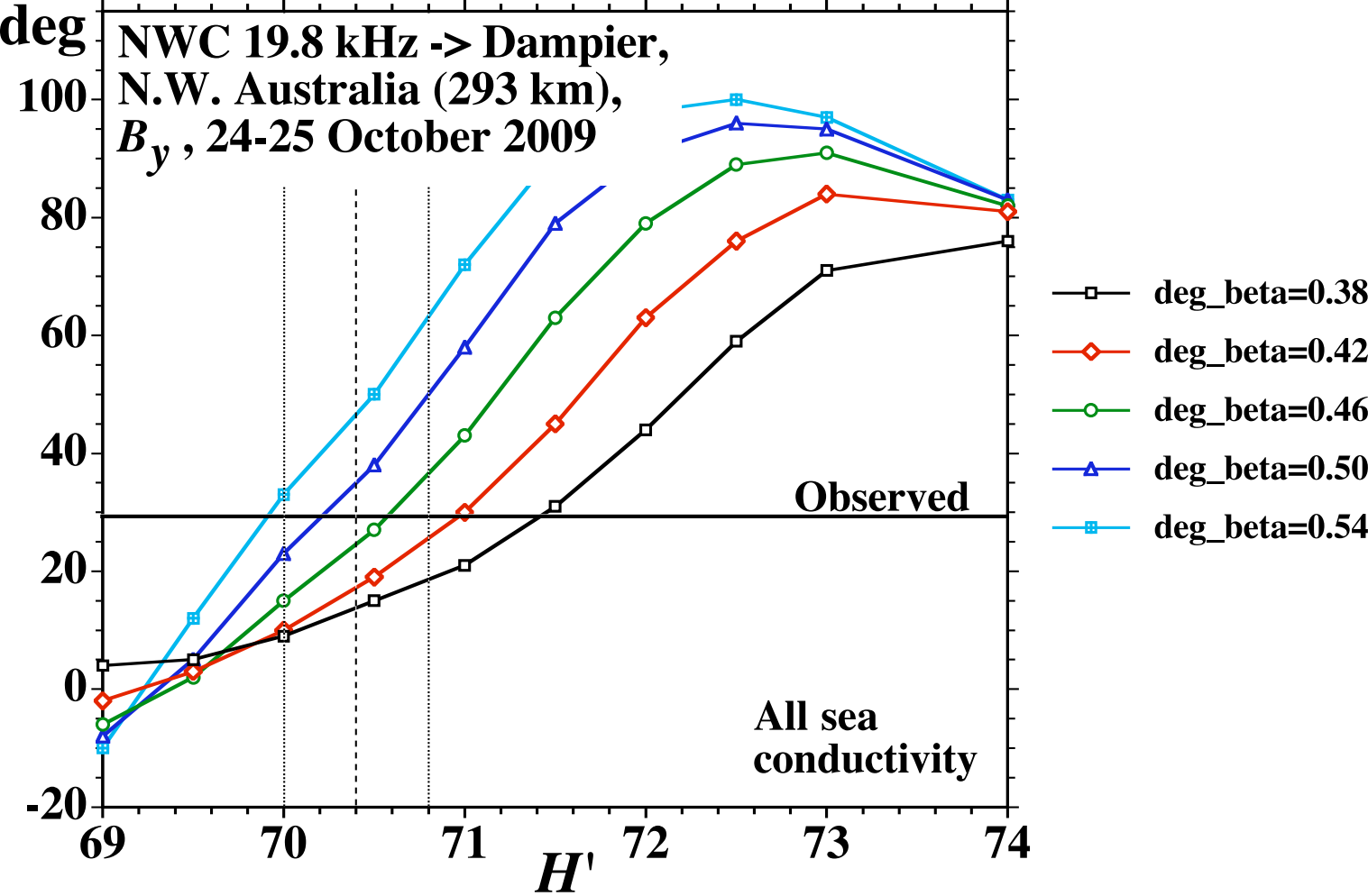
deg
NWC 19.8 kHz -> Dampier,
N.W. Australia (293 km),
B_y , 24-25 October 2009
100
80
60
40
20
0
-20
Observed
All sea
conductivity
69
70
71
72
73
74
H'
deg_beta=0.38
deg_beta=0.42
deg_beta=0.46
deg_beta=0.50
deg_beta=0.54

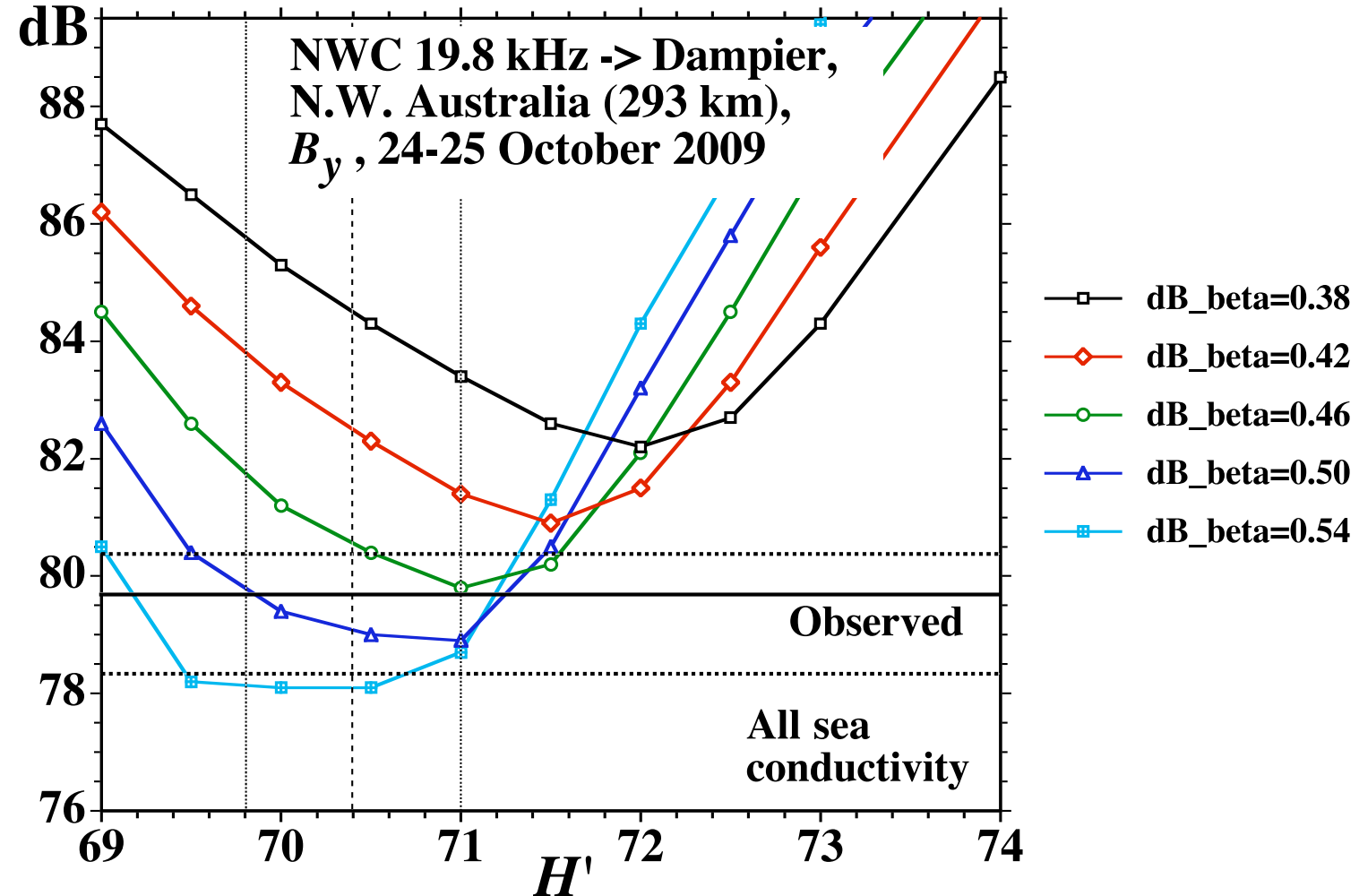
dB
NWC 19.8 kHz -> Dampier,
N.W. Australia (293 km),
B_y , 24-25 October 2009
88
86
84
82
80
78
76
Observed
All sea
conductivity
69
70
71
72
73
74
H'
dB_beta=0.38
dB_beta=0.42
dB_beta=0.46
dB_beta=0.50
dB_beta=0.54

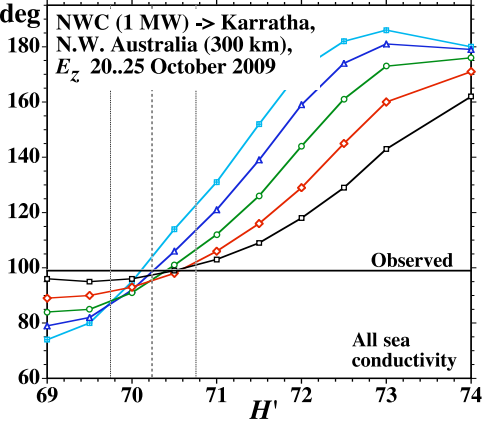
deg
NWC (1 MW) -> Karratha,
N.W. Australia (300 km),
E_z 20..25 October 2009
deg_beta=0.38
deg_beta=0.42
deg_beta=0.46
deg_beta=0.50
deg_beta=0.54
Observed
All sea
conductivity
H'

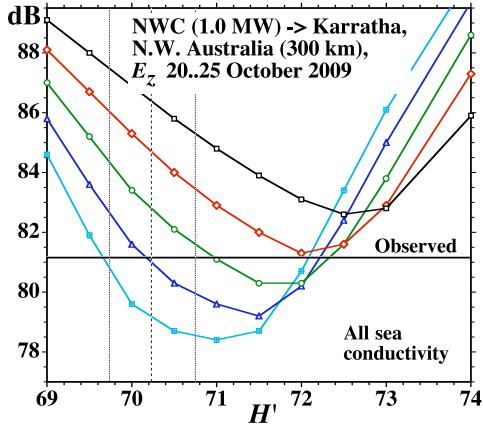
dB
NWC (1.0 MW) -> Karratha,
N.W. Australia (300 km),
E_z 20..25 October 2009
dB_beta=0.38
dB_beta=0.42
dB_beta=0.46
dB_beta=0.50
dB_beta=0.54
Observed
All sea
conductivity
H'

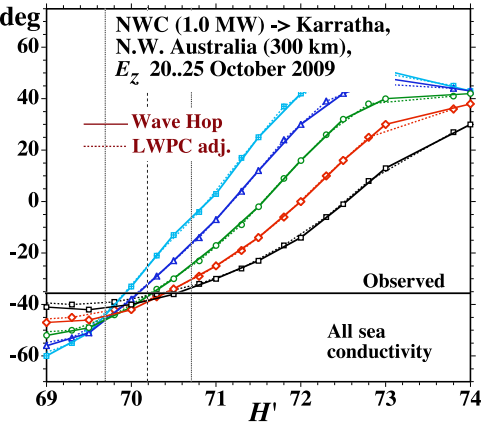
deg
NWC (1.0 MW) -> Karratha,
N.W. Australia (300 km),
E_z 20..25 October 2009
Wave Hop
LWPC adj.
Observed
All sea
conductivity
H'

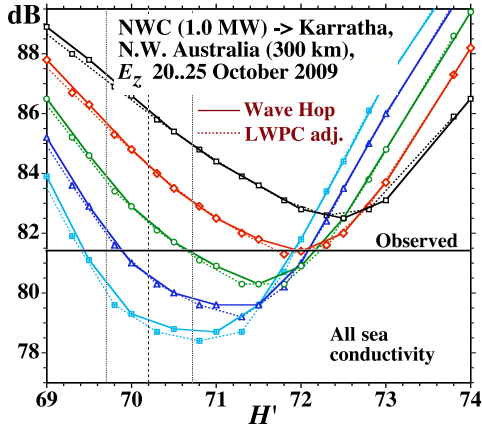
dB
NWC (1.0 MW) -> Karratha,
N.W. Australia (300 km),
E_z 20..25 October 2009
Wave Hop
LWPC adj.
Observed
All sea
conductivity
H'

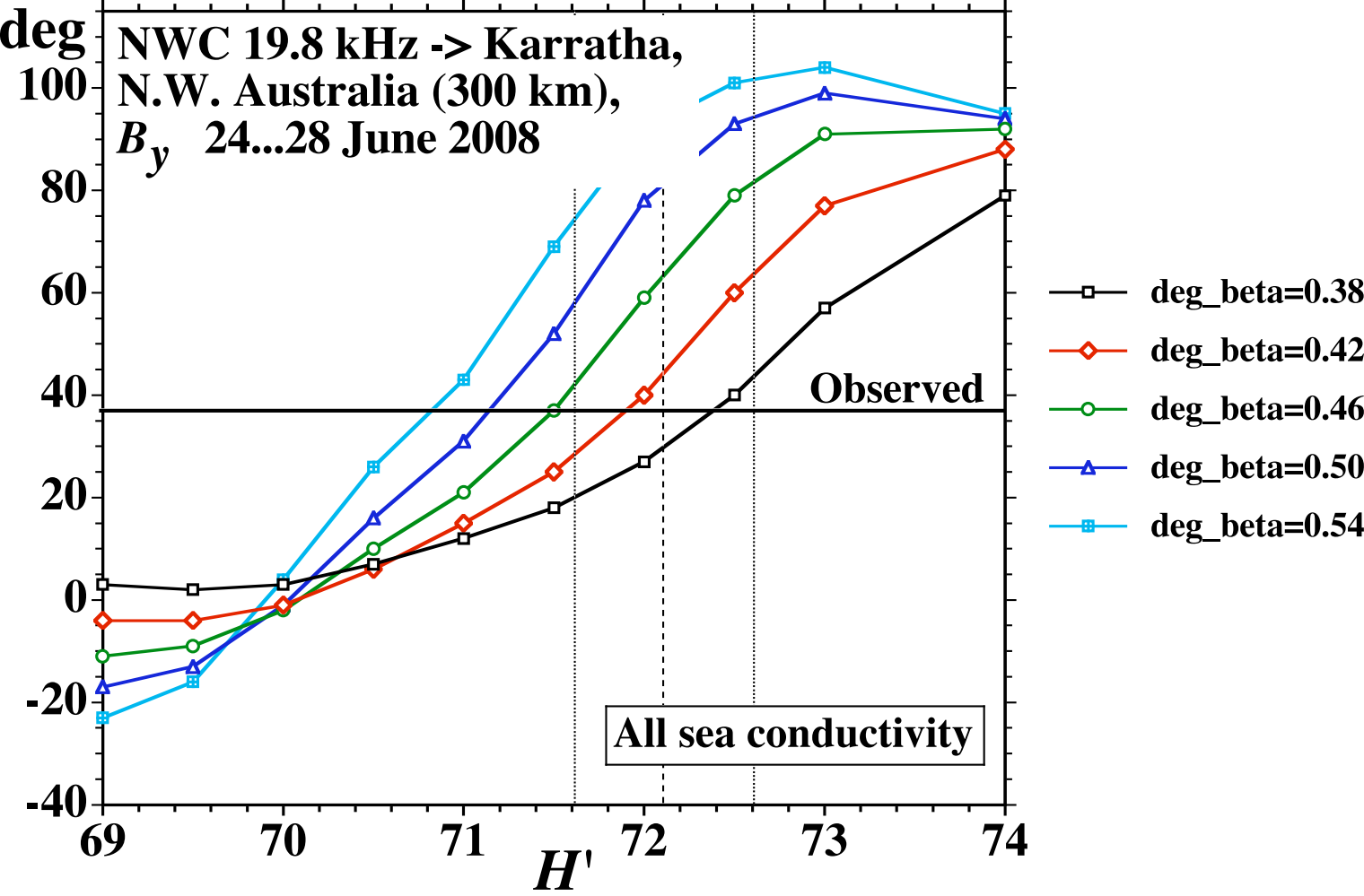
deg
NWC 19.8 kHz -> Karratha,
N.W. Australia (300 km),
B_y 24...28 June 2008
Observed
All sea conductivity
deg_beta=0.38
deg_beta=0.42
deg_beta=0.46
deg_beta=0.50
deg_beta=0.54
100
80
60
40
20
0
-20
-40
69
70
71
72
73
74
H'

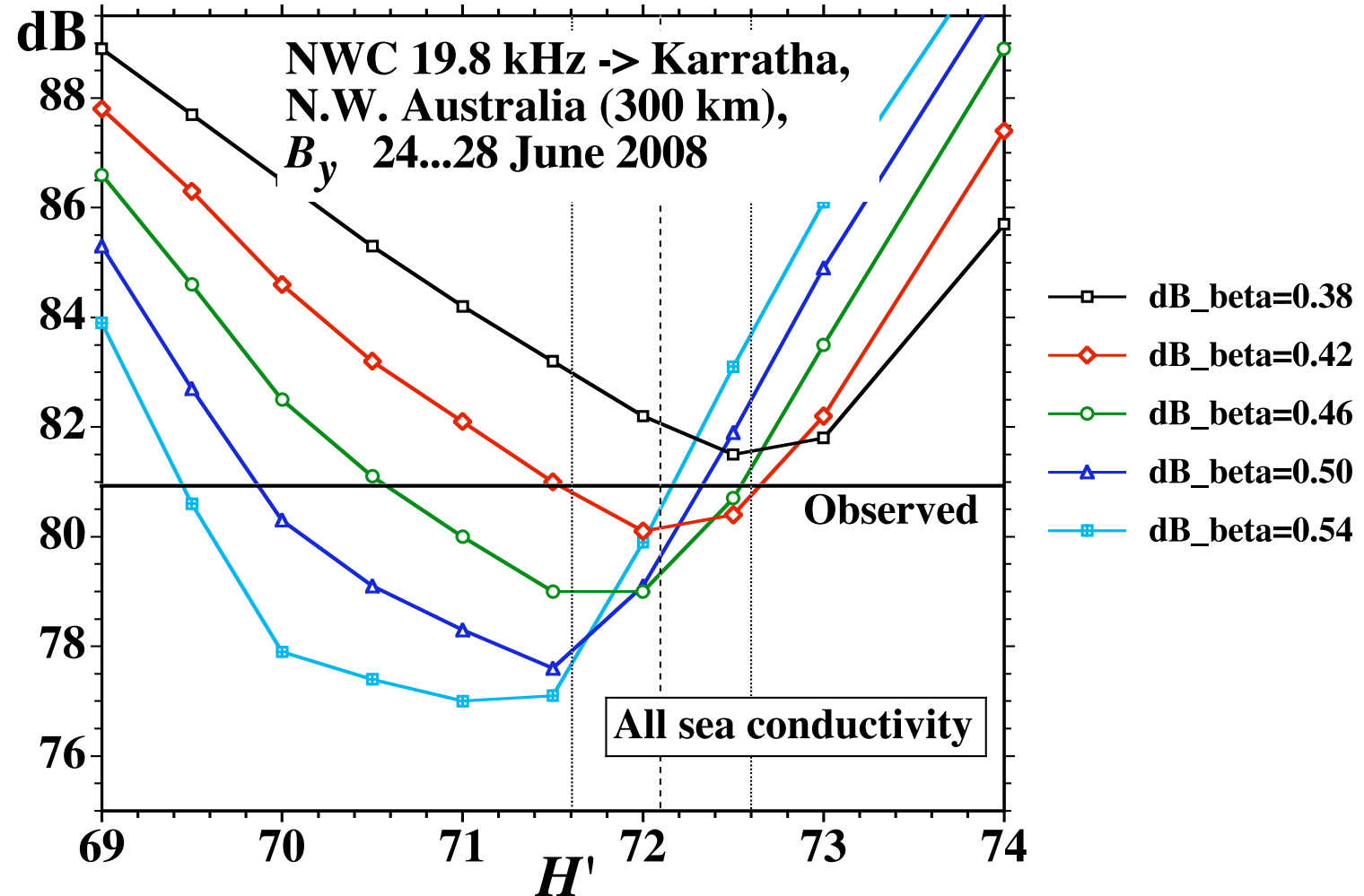
dB
NWC 19.8 kHz -> Karratha,
N.W. Australia (300 km),
B_y 24...28 June 2008
Observed
All sea conductivity
dB_beta=0.38
dB_beta=0.42
dB_beta=0.46
dB_beta=0.50
dB_beta=0.54
88
86
84
82
80
78
76
69
70
71
72
73
74
H'